

Crystal Structures of Dialkylglycine Decarboxylase Inhibitor Complexes

Vladimir N. Malashkevich^{1*}, Pavel Strop¹, John W. Keller²
 Johan. N. Jansonius¹ and Michael D. Toney^{3*}

¹Department of Structural Biology, Biozentrum University of Basel Klingelbergstrasse 70 4056 Basel, Switzerland

²Department of Chemistry University of Alaska-Fairbanks USA

³Department of Chemistry University of California-Davis One Shields Avenue, Davis CA 95616, USA

The crystal structures of four inhibitor complexes of dialkylglycine decarboxylase are reported. The enzyme does not undergo a domain closure, as does aspartate aminotransferase, upon inhibitor binding. Two active-site conformations have been observed in previous structures that differ in alkali metal ion content, and two active-site conformations have been shown to coexist in solution when a single type of metal ion is present. There is no indication of coexisting conformers in the structures reported here or in the previously reported structures, and the observed conformation is that expected based on the presence of potassium in the enzyme. Thus, although two active-site conformations coexist in solution, a single conformation, corresponding to the more active enzyme, predominates in the crystal. The structure of 1-aminocyclopropane-1-carboxylate bound in the active site shows the aldimine double bond to the pyridoxal phosphate cofactor to be fully out of the plane of the coenzyme ring, whereas the C α -CO $_2^-$ bond lies close to it. This provides an explanation for the observed lack of decarboxylation reactivity with this amino acid. The carboxylate groups of both 1-aminocyclopropane-1-carboxylate and 5'-phosphopyridoxyl-2-methylalanine interact with Ser215 and Arg406 as previously proposed. This demonstrates structurally that alternative binding modes, which constitute substrate inhibition, occur in the decarboxylation half-reaction. The structures of D and L-cycloserine bound to the active-site show that the L-isomer is deprotonated at C $^{\alpha}$, presumably by Lys272, while the D-isomer is not. This difference explains the ~3000-fold greater potency of the L *versus* the D-isomer as a competitive inhibitor of dialkylglycine decarboxylase.

© 1999 Academic Press

Keywords: X-ray crystallography; inhibitor complexes; catalytic mechanism; structure

*Corresponding authors

Introduction

Dialkylglycine decarboxylase (DGD) is an unusual PLP-dependent enzyme that catalyzes a decarboxylation-dependent transamination reaction

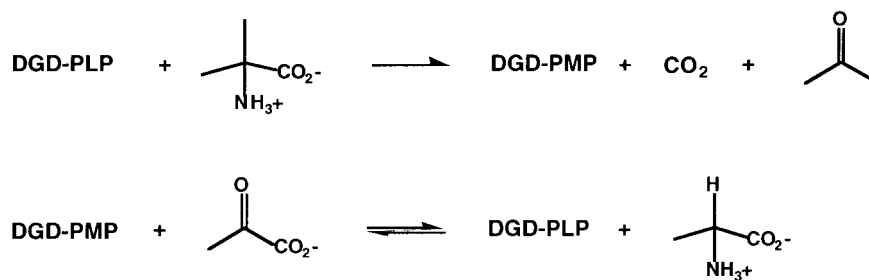
Present addresses: V. N. Malashkevich, Whitehead Institute for Biomedical Research, Massachusetts Institute of Technology; P. Strop, Department of Biochemistry, California Institute of Technology.

Abbreviations used: DGD, 2,2-dialkylglycine decarboxylase; PLP, pyridoxal 5'-phosphate; ACC, 1-amino-1-cyclopropane carboxylate; PPL-MeAla, 5'-phosphopyridoxyl-2-methylalanine; L-cSer, L-cycloserine; D-cSer, D-cycloserine; P-MeAla, phosphono-2-methylalanine.

E-mail addresses of the corresponding authors: malashkevich@wi.mit.edu; mdtoney@ucdavis.edu

between dialkylglycines, e.g. 2-aminoisobutyrate (2-methylalanine) and pyruvate. Aminoisobutyrate is oxidatively decarboxylated to yield CO $_2$ and acetone with the amino group being transferred to the coenzyme. The resulting pyridoxamine-5'-phosphate form of the enzyme then undergoes a classical transamination reaction with pyruvate to give L-alanine and the regenerated PLP-enzyme form.

The structures of four forms of the enzyme differing in alkali metal ion content have been solved (Hohenester *et al.*, 1994). These structures show that the enzyme undergoes a two-state metal ion size-dependent switch in conformation with the Li $^+$ and Na $^+$ forms having one structure and the K $^+$ and Rb $^+$ forms having another. In solution, Li $^+$ and Na $^+$ inhibit the enzyme, while K $^+$ and Rb $^+$ activate it. Zhou *et al.* (1998) demonstrated that



Scheme 1.

two active-site conformations of the enzyme, differing in activity, coexist in solution. The conformational equilibrium between these two forms depends on the identity of the alkali metal ion present, suggesting that the two forms in solution correspond to those observed in the crystal structures. The conformational equilibrium in solution is shifted towards the less active, tighter binding form when substrates or inhibitors are present.

Aminotransferases have been divided into four distinct evolutionary subgroups by Christen's group (Mehta *et al.*, 1993). DGD belongs to the aminotransferase subgroup II, even though it catalyzes a decarboxylation reaction. Recently, the structures of two other subgroup II aminotransferases, glutamate-1-semialdehyde aminomutase (Hennig *et al.*, 1997) and ornithine aminotransferase (Shen *et al.*, 1998), have been reported, including inhibitor-bound forms for the latter (Shah *et al.*, 1997; Storici *et al.*, 1999). The binding of inhibitors to these enzymes does not cause large-scale conformational changes, in contrast to what is observed with the well-studied PLP-dependent enzyme aspartate aminotransferase, which belongs to aminotransferase subgroup I.

Here, we report the structures of four different inhibitors bound to the potassium-liganded form of DGD. These structures were determined in order to establish the specific active-site interactions that substrates make with the enzyme, providing a foundation for mutagenesis experiments aimed at delineating the reaction mechanism. These structures also allow the above-mentioned questions concerning conformational changes to be addressed.

Results and Discussion

Lack of domain closure and conformational changes in the liganded enzyme

Figure 1 shows the chemical structures of the four inhibitors used in this study. The crystal absorption spectra of the four inhibitor complexes (data not shown) all show changes from the spectrum of the parent, Mes-liganded structure. These data clearly demonstrate that the inhibitors are bound to the active site and that the binding site is fully occupied.

The well-studied PLP-dependent enzyme aspartate aminotransferase undergoes a large conformational change when substrates or inhibitors bind in the active site (McPhalen *et al.*, 1992). This change can be approximately described as a 13° rotation of the small domain towards the large one, sequestering the substrate or inhibitor from bulk solvent. A similar effect might occur with the related enzyme DGD.

The overlay of the C α traces for the four structures reported here as well as that of the previously reported DGD-K⁺ structure are shown in Figure 2(a). They are extremely similar, with no noteworthy difference. A comparison of these structures to that of the unliganded enzyme (V.N.M. & J.N. J., unpublished results) also shows

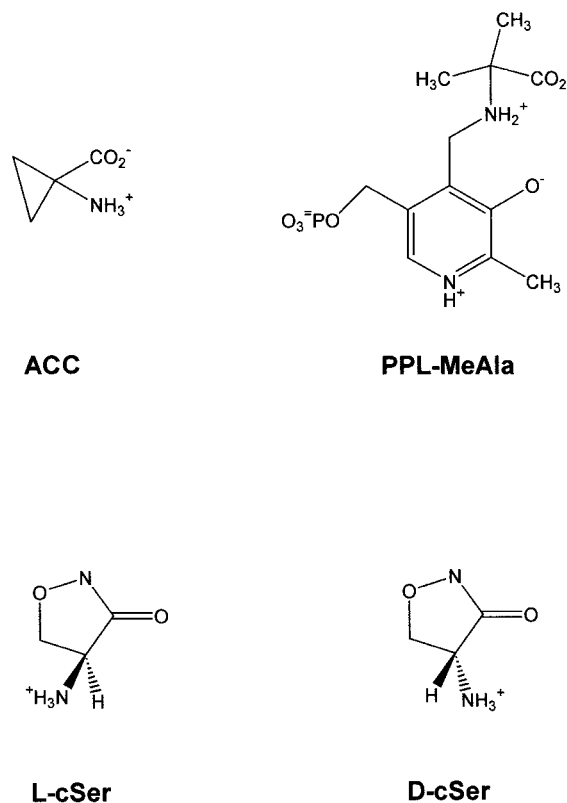


Figure 1. Chemical structures of the inhibitors employed in this study.

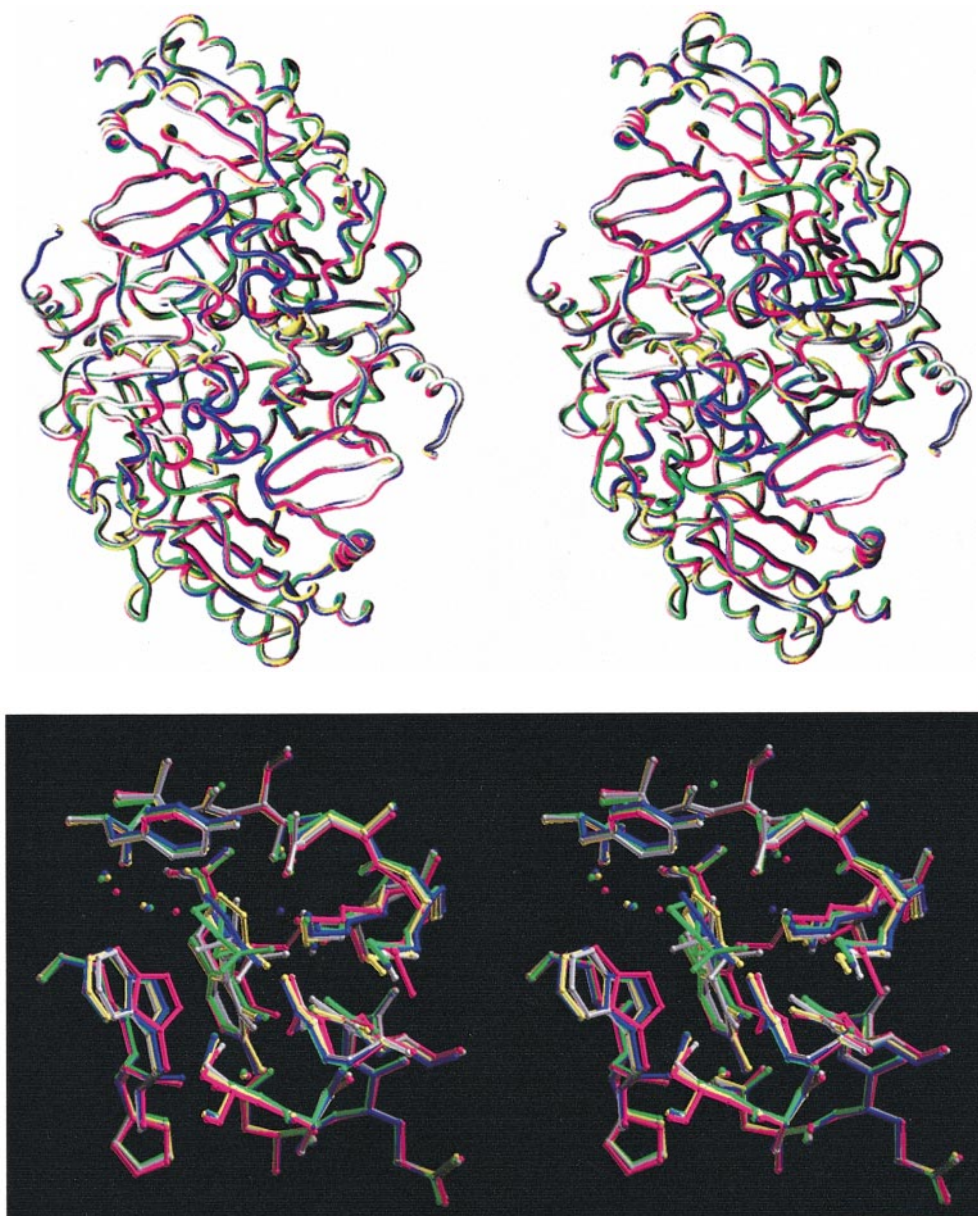


Figure 2. (a) Backbone overlay for the four inhibitor-liganded structures presented here (gray, PPL-MeAla; green, ACC; blue, L-cSer; yellow, D-cSer) along with that of the Mes-liganded structure (magenta) previously reported (Toney *et al.*, 1993). (b) Overlay of the active-site region of the four inhibitor bound structures presented here. Note the absence of significant structural difference in the overall structure or in the active-site region.

no significant conformational changes. Figure 2(b) presents an overlay of the active-site structures of the four inhibitor complexes. As in the C^α traces, the active site shows no significant difference, except in the structures of the inhibitors. Thus, unlike aspartate aminotransferase, DGD does not undergo domain closure on binding substrates or inhibitors.

Shah *et al.* (1997) and Storici *et al.* (1999) found that ornithine aminotransferase, another member of aminotransferase subgroup II (Mehta & Christen, 1994), and whose fold is virtually identical with that of DGD, does not undergo a domain closure when a substrate analogue or inhibitor is

bound. No domain closure was detected in another member of the aminotransferase subgroup II, glutamate-1-semialdehyde aminotransferase (Hennig *et al.*, 1997). Rather, this latter enzyme has a mobile loop formed by residues 153-181 that closes over the active site when substrate binds. Given this series of observations, it is reasonable to suggest that the lack of a domain closure upon substrate binding is a general feature of the enzymes that constitute aminotransferase subgroup II.

Zhou *et al.* (1998) found that DGD coexists as two active-site conformations in solution when a single type of alkali metal ion is present, and that the equilibrium between these isomers shifts

towards the less active form in the presence of substrates or inhibitors. This less active form presumably has the active-site structure of the Na⁺-liganded form observed in the crystal structure, while the more active form presumably has the active-site structure of the K⁺-liganded form, since Na⁺ inhibits and K⁺ activates the enzyme. The crystallization and stabilization buffers used here were the same as those that previously produced DGD-K⁺. The refined structures are also entirely consistent with this form of the enzyme, with no indication of a mixed population of conformers. Thus, even though substrate or inhibitor binding in solution causes a shift of at least the active-site structure towards that of the DGD-Na⁺ conformation, it does not do so in the crystal. This is remarkable, given that DGD-K⁺ and DGD-Na⁺ are readily interconvertible in the crystal (Hohenester *et al.*, 1994).

Coenzyme tilt angle

The internal aldimine formed between Lys272 and the coenzyme C4' is, by extrapolation from studies on other aminotransferases (Toney & Kirsch, 1993), necessary for rapid formation of the external aldimine by providing a transamination pathway. The geometric constraints of the internal Schiff base linkage determine the tilt angle of the coenzyme in the unliganded (or Mes-liganded) enzyme. External aldimine formation, the first obligatory chemical step in the DGD reaction, necessarily causes a coenzyme reorientation so that steric clashes between Lys272 and the substrate Schiff base are avoided. The coenzyme reorientations observed for all four structures presented here are very similar, as seen in the overlay of the active-site structures presented in Figure 2(b). The coenzyme in the ACC structure tilts ~13° forward with respect to the coenzyme in the internal aldimine

structure (Figure 3). This is smaller than the 18°–25° rotation seen in ornithine aminotransferase (Shah *et al.*, 1997; Storici *et al.*, 1999). The structures of the four inhibitors employed here (Figure 1) are quite disparate, as are their specific modes of interaction with the active site. This suggests that there is a specific structural reason for the very similar coenzyme tilt angles in the four structures presented.

One explanation for the uniformity in coenzyme tilt angle is that strong restraints are placed on the indole group of Trp138, which forms the front of the substrate binding pocket. It makes steric interactions with SD of Met141 and OG of Ser151 that restrict the benzene moiety of the indole group. The indole nitrogen atom makes an intimate hydrogen bond with a water molecule (Wat513) that bridges Trp138 and the phosphate oxygen atom. This water molecule makes two additional hydrogen bonding interactions with the main-chain carbonyl group of Tyr301 and a second water molecule, saturating its potential and rigidly fixing it. Further forward tilting of the coenzyme would likely require breaking this strong (~2.8 Å) hydrogen bond made to Wat513 by the indole nitrogen atom as well as rearrangement of the Met141 and Ser151 side-chains. Wat513 is observed in all three of the higher-resolution structures reported here.

ACC and PPL-MeAla structures

Figure 4 presents an overlay of the ACC and PPL-MeAla active-site structures. Hydrogen bonding interactions of 3.0 Å or less are shown as broken lines for the ACC structure. Arg406 makes a hydrogen bonding/ionic interaction with the ACC carboxylate group at a distance of 3.0 Å, largely neutralizing its charge. Ser215 makes a strong

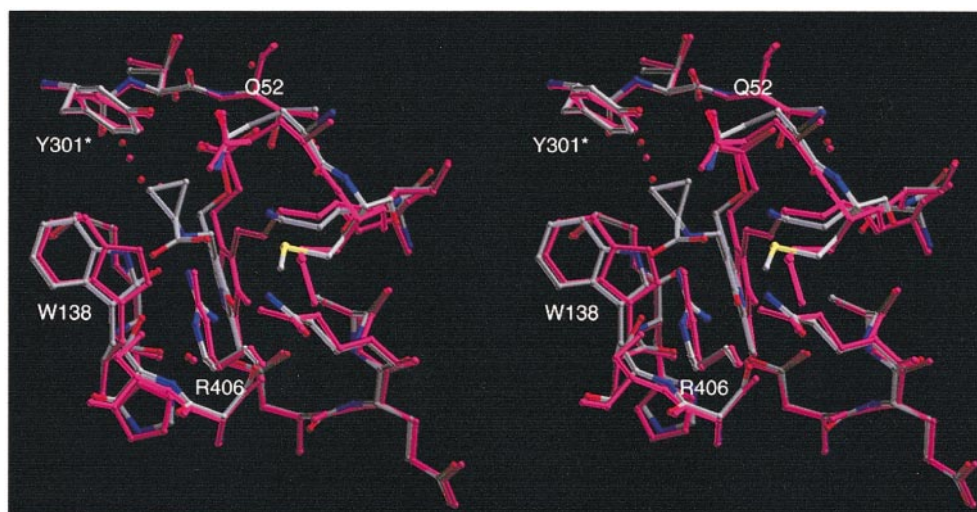


Figure 3. Overlay of the active-site region of the previously solved internal aldimine structure (magenta) and the ACC structure presented here (colored by atom type). Note the ~13° change in the coenzyme tilt angle necessitated by formation of the Schiff base between the inhibitor and coenzyme.

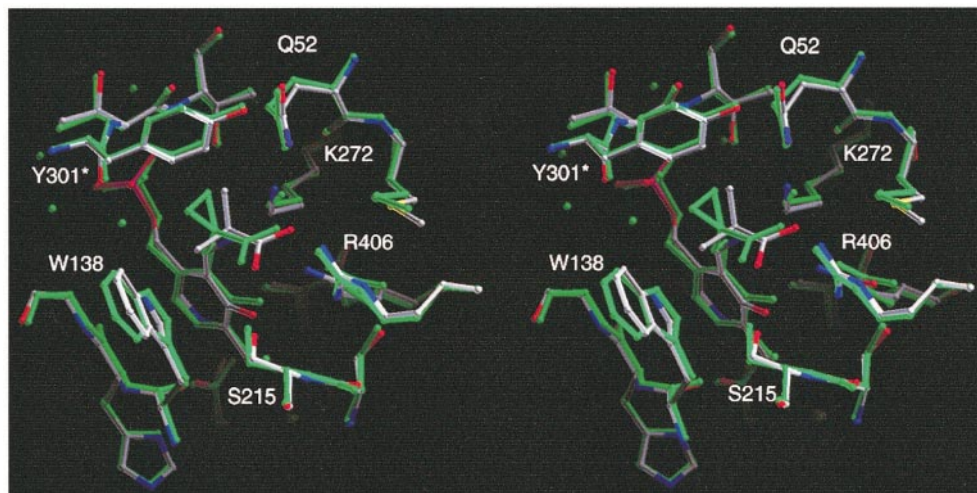


Figure 4. Overlay of the active-site regions for the ACC (green) and PPL-MeAla (colored by atom type) structures. Note the non-planarity of the ACC aldimine with the coenzyme ring. This may be the cause of the lack of decarboxylation reactivity of this amino acid.

(~ 2.6 Å) hydrogen bond to the carboxylate group in both structures.

An unusual feature of the ACC structure is the non-planarity of the Schiff base with the coenzyme ring (Figure 3). The coplanar conformation of the protonated Schiff base is expected to be the most stable, since it allows conjugation with the aromatic ring and hydrogen bonding between it and O3' of the pyridine ring. It is observed in the structure of α -methylaspartate bound to aspartate aminotransferase (McPhalen *et al.*, 1992). Although the structural reason for this Schiff base conformation is not evident, it does explain the lack of decarboxylation reactivity of ACC observed by Sun *et al.* (1998).

In order for decarboxylation to occur, the substrate carboxylate group must be placed in an orientation such that the C^α -CO₂⁻ bond is approximately orthogonal to the plane of the coenzyme ring (i.e. such that the C4'-N-C^α-CO₂⁻ dihedral angle is $\pm 90^\circ$, with the Schiff base coplanar with the ring). This orientation allows the reaction to take advantage of stereoelectronic effects, which were proposed by Dunathan (1966) to play a major role in control of reaction specificity in pyridoxal phosphate-dependent enzymes.

Toney *et al.* (1995) proposed that the DGD active-site has three binding subsites, termed the A, B, and C subsites. The B subsite is that where the carboxylate groups of ACC and PPL-MeAla are observed in the present structures. When the C^α -CO₂⁻ bond is orthogonal to the coenzyme ring plane, the carboxylate group would receive hydrogen bonds from Gln52 and Lys272, and possibly from Arg406. These interactions constitute the A subsite. The C subsite corresponds roughly to the position of the methyl group in the PPL-MeAla structure, near Trp138. Sun *et al.* (1998) validated this binding subsite model by kinetic methods.

They also demonstrated the presence of alternative substrate binding modes in the decarboxylation half-reaction, with the substrate carboxylate group binding preferentially in the B over the A subsite. The ACC and PPL-MeAla structures shown in Figure 4 strongly support the conclusion reached from kinetic experiments, that a substantial fraction of substrate in the decarboxylation reaction is bound non-productively with the carboxylate group in the B subsite. On the other hand, this binding mode is the productive one for the transamination half-reaction catalyzed by DGD, since it would place the C^α-H bond of L-alanine in the A subsite. The fact that there is no indication of a carboxylate group in the A subsite for either structure suggests further that the non-productive binding mode is dominant.

Cycloserine structures

The active-site structures of D and L-cycloserine (Figure 1) are shown in Figure 5. The D-isomer is tetrahedral at C^α, while the L-isomer is planar. The L-isomer of cycloserine presents the labile C-H bond of the oxazole ring to Lys272. This residue has been proposed (Toney *et al.*, 1995) to be the general base catalyst for the transamination half-reaction, based on analogy to other aminotransferases. The observation that L-cycloserine is planar in the present structure (Figure 5) demonstrates that the α -proton has been removed and suggests that a resonance-stabilized structure (most probably ketimine, as suggested by the crystal UV-VIS spectra; V.N.M. & J.N.J, unpublished results; Malashkevich *et al.*, 1993) is present in the active site. Bailey *et al.* (1970) showed that L-cycloserine forms an external aldimine but does not form covalent bonds with active-site side-chains. They found that both isomers are competitive inhibitors.

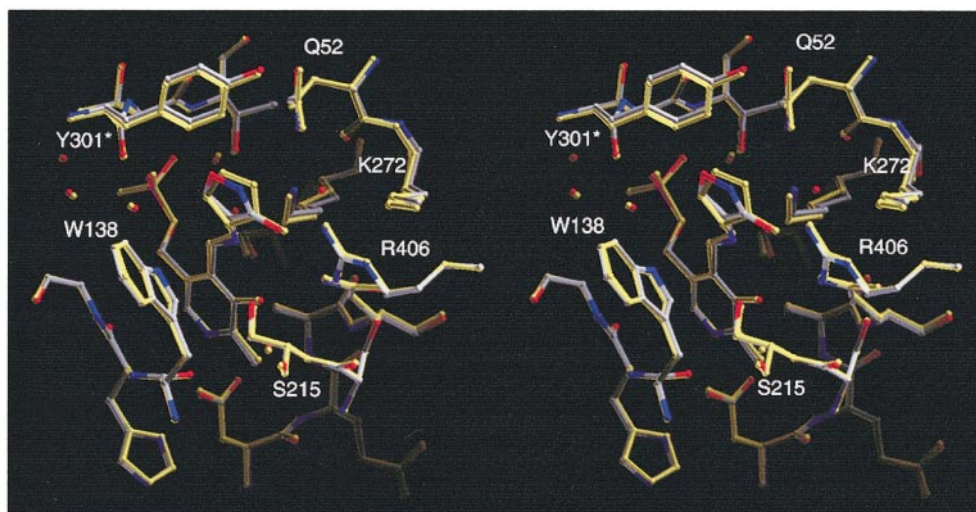


Figure 5. Overlay of the active-site regions for the D (yellow) and L-cycloserine (colored by atom type) structures. The L-isomer is planar at C α while the D-isomer is tetrahedral, indicating that the L-isomer has been deprotonated. No covalent interaction between the inhibitor and enzyme is observed.

The present structures are in agreement with their results.

The difference in geometry at C α has consequences for the hydrogen bonding interactions that the oxazole ring makes. The exocyclic oxygen atoms of both isomers make hydrogen bonding interactions with Arg406. The endocyclic nitrogen atom of the D-isomer accepts a hydrogen bond from Gln52, but the planar geometry of the L-isomer precludes this interaction. The ring of the L-isomer is positioned more forward, due to the planarity at C α caused by deprotonation, allowing a water molecule to enter between the inhibitor and Lys272. This water molecule makes a bridging hydrogen bonding interaction with the Lys272 amino group and the exocyclic oxygen atom of the inhibitor.

Conclusions

The four structures of inhibitors bound to DGD presented here, combined with previous results, provide evidence that DGD, and likely all members of the aminotransferase subgroup II, do not undergo large-scale conformational changes upon inhibitor binding, in contrast to the well-studied aspartate aminotransferase of subgroup I. The active site of DGD shows a remarkable rigidity, in that the coenzyme tilt angle and position are well conserved for inhibitors possessing widely differing structures. The reversibility of inhibition observed previously for both D and L-cycloserine is confirmed here by the absence of covalent interactions between the inhibitors and the enzyme. The L-isomer has been deprotonated, as evidenced by the planar configuration at C α , providing strong support for the proposition that Lys272 is the general base catalyst in the DGD transamination half-reaction and explaining the greater potency, as an inhibitor for DGD, of this isomer.

Experimental Procedures

Materials

DGD was purified as described previously (Sun *et al.*, 1998). Potassium phosphate, sodium pyruvate, PEG4000, Mes, and PLP were from Fluka. PPL-MeAla was synthesized by borohydride reduction of the Schiff base formed between aminoisobutyrate and PLP (Severin *et al.*, 1969). D-cycloserine was from Fluka. 1-Aminocyclopropane-1-carboxylate and L-cycloserine were from Calbiochem.

Crystallization and X-ray diffraction data collection

Crystals of DGD were grown by the hanging drop vapor diffusion method using a modification of the protocol described by Toney *et al.* (1993). Drops of 4 μ l containing 31.5 mg/ml protein, 5 mM potassium phosphate (pH 7.5), 15 μ M PLP, were mixed with 2 μ l of reservoir solution containing 150–200 mM sodium pyruvate (pH 7.7), 15% PEG4000, 30 mM Mes-KOH (pH 6.4), and equilibrated against 1 ml of this reservoir solution. Macroseeding was used to obtain large crystals shaped in the form of hexagonal prisms. The crystals grew to a maximum size of 0.4 mm \times 0.4 mm \times 0.5 mm in two to three weeks. Inhibitors were diffused into these crystals by soaking in a stabilizing solution containing 30% PEG4000, 30 mM Mes-KOH (pH 6.4), and the appropriate inhibitor. The inhibitor concentrations were as follows: 50 mM ACC, 20 mM PPL-MeAla (pH 5.5, in order to effect coenzyme release), 50 mM L-cSer or 50 mM D-cSer.

Diffraction data for the DGD-PPL-MeAla complex were collected at room temperature on a MarResearch (Hamburg, Germany) imaging plate using CuK α radiation. High-resolution data for the other four complexes were collected at 100 K using the synchrotron beamline BW6 of the Max-Planck Gesellschaft at DESY, Hamburg. Crystals were harvested from the stabilizing solution described above containing, in addition, 26% glycerol, and flash-frozen. Reflection intensities were integrated with DENZO, merged together using SCALEPACK (Otwinowski & Minor, 1996), and reduced to structure

Table 1. Data collection and refinement statistics

	PPL-MeAla	ACC	L-cSer	D-cSer
Resolution (Å)	10.0-2.80	10.0-2.00	10.0-1.95	10.0-2.05
R_{sym}^a	0.058	0.049	0.062	0.075
No. of reflections	14,654	42,301	42,043	36,835
Redundancy	4.1	3.9	3.9	4.0
Completeness (%)	96.0	96.6	95.6	97.5
R_{cryst}^b	0.185	0.215	0.193	0.186
No. of protein atoms	3246	3246	3246	3247
No. of solvent atoms	35	151	148	151
No. of heteroatoms	25	25	24	24
Mean <i>B</i> -factor (Å ²)				
Entire molecule	41.8	33.3	35.3	34.7
Main-chain	38.8	29.4	31.3	30.9
Side-chains	41.8	37.8	39.8	39.0
Solvent	60.6	39.4	41.6	42.3
Rmsd from ideality				
Bond distances (Å)	0.012	0.011	0.012	0.011
Bond angles (deg.)	1.62	1.54	1.69	1.60
Planar groups (Å)	0.010	0.011	0.010	0.011

^a $R_{\text{sym}} = \frac{\sum_j |I_j(hkl) - \langle I(hkl) \rangle|}{\sum_j I_j(hkl)}$, where I_j is the intensity measurement for reflection j and $\langle I \rangle$ is the mean intensity over j reflections.

^b $R_{\text{cryst}} = \frac{\sum ||F_{\text{obs}}(hkl)| - |F_{\text{calc}}(hkl)||}{\sum |F_{\text{obs}}(hkl)|}$, where F_{obs} and F_{calc} are observed and calculated structure factors, respectively. No σ -cutoff was applied.

factors using TRUNCATE from the CCP4 (1994) program suite. Data collection statistics are presented in Table 1.

Structure solution and refinement

The structures of the DGD complexes were solved by molecular replacement using the program AMoRe (Navaza, 1994) and the DGD-K⁺ structure (Toney *et al.*, 1993), from which the Mes ligand had been removed, as the search model. Model building and electron density interpretation employed the program O (Jones *et al.*, 1991). The structures were refined (Table 1) using the programs XPLOR (Brünger, 1992) and TNT (Tronrud *et al.*, 1987).

Protein Data Bank accession number

The atomic coordinates have been deposited with the Protein Data Bank, Brookhaven, with accession codes 1D7V, 1D7R, 1D7U and 1D7S for the PPL-MeAla, ACC, L-cSer and D-cSer complexes, respectively.

Acknowledgments

We are grateful to Dr H. Bartunik for providing the beamtime, and to Drs A. Popov and G. Bourenkov at the BW6 beamline for their assistance during data collection. This study was supported in part, by the Swiss National Science Foundation grant 31-36432.92 to J.N.J and the U.S. National Institutes of Health grant GM54779 to M.D.T.

References

Bailey, G. B., Chotamangsa, O. & Vuttivej, K. (1970). Control of pyridoxal phosphate enzyme reaction specificity studied with α -dialkylamino acid transaminase. *Biochemistry*, **9**, 3243-3248.

Brünger, A. T. (1992). *X-PLOR, Version 3.1: A System for Crystallography and NMR*, Yale University Press, New Haven, CT.

Collaborative Computing Project No. 4. (1994). The CCP4 suite: programs for protein crystallography. *Acta Crystallog. sect. D*, **50**, 760-763.

Dunathan, H. C. (1966). Conformation and reaction specificity in pyridoxal phosphate enzymes. *Proc. Natl Acad. Sci. USA*, **55**, 712-716.

Hennig, M., Grimm, B., Contestabile, R., John, R. A. & Jansonius, J. N. (1997). Crystal structure of glutamate-1-semialdehyde aminomutase: an α_2 -dimeric vitamin B₆-dependent enzyme with asymmetry in structure and active-site reactivity. *Proc. Natl Acad. Sci. USA*, **94**, 4866-4871.

Hohenester, E., Keller, J. W. & Jansonius, J. N. (1994). An alkali metal ion size-dependent switch in the active-site structure of dialkylglycine decarboxylase. *Biochemistry*, **33**, 13561-13570.

Jones, T. A., Zou, J.-W., Cowan, S. W. & Kjeldgaard, M. (1991). Improved methods for building protein models in electron density maps and the location of errors in these models. *Acta Crystallog. sect. D*, **47**, 110-119.

Malashkevich, V. N., Toney, M. D. & Jansonius, J. N. (1993). Crystal structures of true enzymatic reaction intermediates: aspartate and glutamate ketimines in aspartate aminotransferase. *Biochemistry*, **32**, 13451-13462.

McPhalen, C. A., Vincent, M. G. & Jansonius, J. N. (1992). X-ray structure refinement and comparison of three forms of mitochondrial aspartate aminotransferase. *J. Mol. Biol.* **227**, 197-213.

Mehta, P. K. & Christen, P. (1994). Homology of 1-aminocyclopropane-1-carboxylate synthase, 8-amino-7-oxononanoate synthase, 2-amino-6-caprolactam racemase, 2,2-dialkylglycine decarboxylase, glutamate-1-semialdehyde aminomutase, and isopenicillin-N-epimerase with aminotransferases. *Biochem. Biophys. Res. Commun.* **198**, 138-143.

Mehta, P. K., Hale, T. I. & Christen, P. (1993). Aminotransferases: demonstration of homology and div-

- ision into evolutionary subgroups. *Eur. J. Biochem.* **214**, 549-561.
- Navaza, J. (1994). AMoRe: an automated package for molecular replacement. *Acta Crystallog. sect. A*, **50**, 157-163.
- Otwinowski, Z. & Minor, W. (1996). Processing of X-ray diffraction data collected in oscillation mode. In *Methods in Enzymology* (Carter, C. W., Jr & Sweet, R. M., eds), vol. 276, pp. 307-325, Academic Press, London.
- Severin, E. S., Gulyeav, N. N., Khurs, E. N. & Khomutov, R. M. (1969). The synthesis and properties of phosphopyridoxyl amino acids. *Biochem. Biophys. Res. Commun.* **35**, 318-323.
- Shah, S. A., Shen, B. W. & Brunger, A. T. (1997). Human ornithine aminotransferase complexed with L-canadine and gabaculine: structural basis for substrate recognition. *Structure*, **5**, 1067-1075.
- Shen, B. W., Hennig, M., Hohenester, E., Jansonius, J. N. & Schirmer, T. (1998). Crystal structure of human recombinant ornithine aminotransferase. *J. Mol. Biol.* **277**, 81-102.
- Storici, P., Capitani, G., Mueller, R., Schirmer, T. & Jansonius, J. N. (1999). Crystal structure of human ornithine aminotransferase complexed with the highly specific and potent inhibitor 5-fluoromethyl-ornithine. *J. Mol. Biol.* **285**, 297-309.
- Sun, S., Zabinski, R. F. & Toney, M. D. (1998). Reactions of alternate substrates demonstrate stereoelectronic control of reactivity in dialkylglycine decarboxylase. *Biochemistry*, **37**, 3865-3875.
- Toney, M. D. & Kirsch, J. F. (1993). Lysine 258 in aspartate aminotransferase: enforcer of the Circe effect for amino acid substrates and general-base catalyst for the 1,3-prototropic shift. *Biochemistry*, **32**, 1471-1479.
- Toney, M. D., Hohenester, E., Cowan, S. W. & Jansonius, J. N. (1993). Dialkylglycine decarboxylase structure: bifunctional active-site and alkali metal sites. *Science*, **261**, 756-759.
- Toney, M. D., Hohenester, E., Keller, J. W. & Jansonius, J. (1995). Structural and mechanistic analysis of two refined crystal structures of the pyridoxal phosphate-dependent enzyme dialkylglycine decarboxylase. *J. Mol. Biol.* **245**, 151-179.
- Tronrud, D. E., Ten, Eyck L. F. & Matthews, B. W. (1987). An efficient general-purpose least-squares refinement program for macromolecular structures. *Acta Crystallog. sect. A*, **43**, 489-501.
- Zhou, X., Kay, S. & Toney, M. D. (1998). Coexisting kinetically distinguishable forms of dialkylglycine decarboxylase engendered by alkali metal ions. *Biochemistry*, **37**, 5761-5769.

Edited by R. Huber

(Received 25 May 1999; received in revised form 23 September 1999; accepted 28 September 1999)